

SKB

**TECHNICAL
REPORT**

87-13

Shallow reflection seismic investigation of fracture zones in the Finnsjö area, method evaluation

Trine Dahl-Jensen
Jonas Lindgren

University of Uppsala, Department of Geophysics
June 1987

SHALLOW REFLECTION SEISMIC INVESTIGATION OF FRACTURE
ZONES IN THE FINNSJÖ AREA, METHOD EVALUATION

Trine Dahl-Jensen
Jonas Lindgren

Uppsala University, Department of Geophysics,
Sweden

June 1987

This report concerns a study which was conducted for SKB. The conclusions and viewpoints presented in the report are those of the author(s) and do not necessarily coincide with those of the client.

Information on KBS technical reports from 1977-1978 (TR 121), 1979 (TR 79-28), 1980 (TR 80-26), 1981 (TR 81-17), 1982 (TR 82-28), 1983 (TR 83-77), 1984 (TR 85-01), 1985 (TR 85-20) and 1986 (TR 86-31) is available through SKB.



UPPSALA UNIVERSITET
INSTITUTIONEN FÖR GEOFYSIK
Avdelningen för fasta jordens fysik

**SHALLOW REFLECTION SEISMIC INVESTIGATION OF
FRACTURE ZONES IN THE FINNSJO AREA
METHOD EVALUATION**

**TRINE DAHL-JENSEN
JONAS LINDGREN**

JUNE 1987

Uppsala Universitet
Department of Geophysics
Section of Solid Earth Geophysics
Box 556 S-751 22 Uppsala
Sweden

Abstract

In the Finnsjö area a reflection seismic profile has been shot. Under the profile the crystalline bedrock lies close to the surface (seldom more than 2 m) , and the seismic velocities are high. There are known fracture zones in the area. A larger, sub horizontal fracture zone (zone 2) turned out to be difficult to detect, while a steeply dipping zone (Brändan zone) seems to be more reflective. It has not been possible to present a stacked section that enhances zone 2 so it can be followed along the profile. A reason can be that it simply is not a very reflective zone.

T A B L E O F C O N T E N T S

<u>Section</u>	<u>Page</u>
1 Orientation	3
2 Field parameters	3
3 Expected features on a shotgather	4
4 Can we see zone 2 ?	4
5 The shot sections	5
6 Overveiw of the processing of the data	6
7 Frequency Filtering	7
8 Stacking Velocity	8
9 Semblance Analysis	9
10 Mute Stacking	10
11 Frequency-wavenumber filtering (FK-filtering)	11
12 Deep stack	13
13 Summary and conclusions	14

1 Orientation

In april and may 1987 a reflection seismic pre-test and a 2130 m long profile was recorded in the Finnsjö area, corresponding to a subsurface coverage of 1700 m (fig. 1). The purpose was to see if reflection seismic profiling can be used to detect horizontal (or near horizontal) fracture zones, at fairly shallow depths (from 50 m to a few km).

The crystalline bedrock lies close to the surface underneath the profile, and nearly all shots along the profile were drilled into bedrock. The seismic velocities are known from Ahlbom et al. to be high close to the surface.

In the Finnsjö area there are (at least) 2 known fracture zones, the steeply dipping Brändan fracture zone, and a more gently dipping zone, referred to as zone 2 (Ahlbom et al.). The profile is placed perpendicular to the strike of zone 2. At one end of the profile the zone is estimated to be at a depth of 50 m, and in the other at a depth of approximatly 400 m.

2 Field parameters

The test area was positioned near Fi7 and the data from the shot sections from this area was used to determine the setup for the profile. Fig. 1 shows the area. A total of 151 shots of 50 g of explosives were fired in drilled holes with 10 m spacing. The boreholes were tamped with water or sand before firing. Each shot was recorded on 60 28 Hz single geophones, with offset ranging from 100 m to 790 m.

Nearly all shots were fired in bedrock (Ekman & Jacobsson 1987) .
However, the depth into bedrock varied, depending on the cover.

Field parameters for shallow reflection seismic profiling (for a
sedimentary ground) are discussed in Knapp and Steeples 1986.

3 Expected features on a shotgather

A shotgather will contain (fig. 2):

- a direct wave (pressure wave) (vel 5.2-5.5 km/s)
- an S-wave (shear wave) (vel 3.0-3.3 km/s)
- a surface wave (vel 2.0-2.4 km/s)
- a ground coupled airblast (vel 340 m/s)

All these different arrivals can possibly interfere with the sought
reflection, so it is necessary to identify them on the
shotsections, and then choose the recording parameters in order to
enhance the reflection as much as possible.

Zone 2 lies between 50 and 400 m under the profile. Assuming constant
velocity down to zone 2 it should appear as a hyperbola.

4 Can we see zone 2 ?

Since the approximate thickness of zone 2 is known (Ahlbom et al.),
the expected frequency content of the reflection signal can be
estimated. Assuming a thickness of 70 meters and a velocity of 5.5
km/s which is the velocity of the direct wave and considering phase
shifts, the expected frequencies should be approximately $(2N + 1) * 20$

Hz, $N = 0,1,2\dots$. This means that the signal can not be separated from unwanted signals by simple frequency filtering.

The amplitude of the signal depends on the difference in acoustic impedance (velocity and density) between the zone and the surrounding rock. Information about these parameters can be used to estimate the strength of a reflected signal.

5 The shot sections

Comparing the shot sections from the profile (fig. 3) with the sections from the test profile recorded in may 1987 (Dahl-Jensen & Palm 1987), it is clear that the quality of the data is more varying. Shots are fired in up to 2 m of bedrock as well as in 4 m soil. The geophone sites have also shown highly varying quality, due to variations in ground conditions.

In the shotsections, a marked difference can be seen between explosions in boreholes mainly drilled in bedrock, and boreholes drilled in soil. Fig. 3 (a), (b) shows two shots fired only 10 meters apart. 59 of the 60 recording geophones were the same.

A shot deeper into bedrock will generate higher frequency energy, while a shot in less than 50 cm bedrock will generate mainly low frequency energy and a pronounced surface wave. The latter will cause trouble in the processing due to the high amplitude.

A shot section from the very beginning of the profile is shown in fig. 3 (c). Zone 2 is here very close to the surface, and the assumed reflection closely interferes with the direct wave. In the processing, there can be problems separating reflectors at this depth (50 - 100 m) from the direct wave.

Figs. 3 (d) and (e) are examples of shot gathers from the central part of the profile. Here, the reflections from zone 2 are very weak and can not be defined with any accuracy without further processing.

A shot section from the end part of the profile is shown in fig. 3 (f). Here, the assumed reflections at geophones closer to the shot are obscured by the S- and the surface-wave

Finally, fig. 3 (g) is a clear example of a shot section where energy, reflected from the steeply dipping Brändan fracture zone, zone 1, appears. Since the dip of the zone is approximately 75° towards East, energy reflected from the fracture zone should appear in shot sections from the part of the profile situated to the East of the zone.

6 Overview of the processing of the data

To enhance the rather weak reflections from zone 2 as seen on the shot sections and to obtain a picture of zone 2, and other possible reflectors under the profile, several approaches have been taken.

CDP-stacking (Hatton et al. 1986) involves the addition of a number of traces recorded on different recording sites and from different shots, after correction for varying offset (NMO-correction, see fig.4). The NMO correction is done under the assumption of straight raypaths and no lateral variation within the CDP-gather, which means that the offset cannot be too large, relatively to the depth of the sought reflector. Also with rather large offset compared to the reflector depth, the velocity used to NMO-correct the data is important. This procedure enhances horizontal (or near horizontal) events, and degrades sloping events (surface- and S-waves).

An effect of NMO-correction of data at shallow depth is frequency distortion. The NMO-correction is often called a dynamic correction, meaning that the correction varies with time. At shallow depths, the signal will be stretched, thus signals containing similar frequencies before NMO will after NMO contain lower frequencies at large offsets. In fig. 5 an example of frequency distortion is shown. To avoid this problem a stack using semblance along hyperbolas is calculated directly on the shot sections without any NMO-correction applied.

In the data from Finnsjön profile 1 the surface- and S-waves have high amplitude compared with the reflected signal from zone 2. If these high amplitude signals aren't dealt with before stacking, they will degrade the stack seriously in the upper 3-400 ms, where the reflection from zone 2 is expected.

To enhance the upper part the data has been muted (unwanted parts of the data zeroed) to remove the direct wave, the surface wave and the S-wave before stacking, leaving behind data where the reflection is undisturbed.

By muting, not only the unwanted events are removed. Where the surface- and S-wave overlies the reflection it is also removed. An approach where only the unwanted events are removed is frequency-wavenumber (FK) filtering of the shot sections. (Hatton et al. 1986) FK-filtering removes only certain dips (velocities) in the data, and can thus be set to remove only the surface- and S-waves, leaving behind the reflection underneath. The shot sections can be stacked after FK-filtering to produce a stacked section.

A stacked section that concentrates on two way travel times (TWT) larger than 400 ms has also been produced.

7 Frequency Filtering

One of the first steps of seismic data processing is frequency filtering, removing energy of unwanted frequencies and saving frequencies corresponding to the reflections. There are two procedures applied to the data, band-pass and notch filtering.

Due to the fact that the data is sampled, a high-cut filter is applied in the field before the data is converted from analog to digital form to avoid aliasing. The data can then be filtered in order to keep only a defined frequency band, in which the reflection events are to be situated.

If currents are flowing in the neighbourhood, and the ground is wet, disturbances can occur due to leakage, with frequencies $N * 50$ Hz, $N = 1, 2, 3, \dots$. In order to remove these frequencies, notch filters can be applied, rejecting only a narrow frequency band centered at the unwanted frequency.

In the Finnsjö data some geophone sites have been strongly contaminated with mainly 150 and 250 Hz. Fig. 6 shows the frequency content of some traces before and after notch filters of the corresponding frequencies have been applied.

8 Stacking Velocity

If the stacking procedure is to work properly, a correct stacking velocity must be defined. For a horizontal reflector bounding a homogeneous and isotropic medium, the stacking velocity should be equal to the velocity in the medium for the wave. If the velocity varies with depth only, a RMS (Root Mean Square) velocity should be chosen. Problems can occur due to inhomogenities in the medium resulting in a variable wave velocity along the profile.

Problems also arise due to dipping reflectors, and reflectors with curvature. It can be shown (Hubral and Krey 1980) that a dipping reflector will require a stacking velocity that is higher than the wave velocity in the medium, independent of the direction of the dip.

To the first approximation, the stacking velocity can be defined as the velocity of the direct wave, assuming that a P-wave reflector is sought. This velocity can be picked from the shot sections. A better velocity can be found assuming a dip of the reflector and correcting the velocity according to the magnitude of the dip.

The correct velocity can also be found by semblance analysis (see below).

9 Semblance Analysis

The semblance of M traces, considering a time window of N samples, where a_{nm} is the amplitude of trace m at time step n , is defined as:

$$C = \frac{\sum_{n=1}^N \left[\sum_{m=1}^M a_{nm} \right]^2}{M \sum_{n=1}^N \sum_{m=1}^M a_{nm}^2}, \quad 0 \leq C \leq 1$$

This is a measure of the similarity between traces. Semblance analysis can be applied to e.g. traces belonging to the same CDP-point. A reflection hyperbola is analytically calculated as a function of velocity and depth, and the semblance is taken along the hyperbola over some window. If the right velocity and depth is found, the signals in the windows should align, and the semblance will show a maximum. The semblance for different CDP-points for a certain velocity can be displayed, and the presence of reflectors can be determined

The semblance function is sensitive to variations in amplitude, frequency and phase between the compared traces. Although the problem of frequency distortion due to NMO-correction arising in the ordinary stacking procedure is overcome, other problems are present. A window for comparison must be chosen, and the length of the optimum window will vary with the frequency of the sought signal. The offsets in a CDP-gather are comparable to the depth of the reflector. This means that the assumption of near vertical raypaths is seriously violated. Assuming a reflecting zone of constant thickness, the frequency of constructive interference will be a function of offset. Hence, the reflection signal subject to semblance analysis will not have a well-defined frequency, and the semblance will decrease.

An example of a CDP-gather that has been subject to semblance analysis is shown in fig. 7 (a). Here, the semblance as a function of velocity and time (TWT) is displayed. Such plots can be set together, showing a "semblance-stack" for a certain velocity. If the chosen velocity corresponds to the velocity of the direct arrival, it will appear as a very marked event at approximately zero time.

Fig. 7 (b) shows a semblance-stack for a velocity closely corresponding to the direct wave. Apart from the strong direct arrival, there is not much to be seen. The variable intensity of the direct arrival could be a result of the varying P-wave velocity along the profile. However, an interesting feature beneath CDP-points 190 - 270 is worth noting.

Features are seen, dipping towards lower numbers - the opposite direction to zone 2. They are first visible at a depth of approximately 200 m below shotpoint 120. Semblance analysis, performed at a higher velocity (fig. 7 (c)) removes the direct wave, while the features are enhanced. This can be interpreted as a dipping reflector, surfacing near shot point 165. This event has not been detected with other processing methods, and since this is within an area where no bore holes are located, the indication of a reflector should be taken with caution.

10 Mute Stacking

When stacking the traces according to the theory of assumed common depth-points (CDP), noise will hopefully cancel out, while the amplitude of the reflection event will improve. But an unwanted signal such as the surface wave with an amplitude considerably higher than the reflection can cause the method to fail. If the frequency band of the unwanted signal overlaps the frequency band of the reflection, it is not possible to remove the disturbance by simple frequency filtering.

One way to overcome this trouble is simply to "cut away" the unwanted shear- and surface wave, and also the ground coupled air blast, by setting the amplitude of the traces for the critical time interval to zero. The result of such a mute is shown in fig. 8. One disadvantage of the method is that some information about the reflector also is muted away, but the results of the stacking can be improved.

A number of attempts have been made to stack the muted traces without the air blast, the surface and shear-wave, and even without the direct wave, but the results have not been convincing.

11 Frequency-wavenumber filtering (FK-filtering)

FK-filtering means filtering out parts of the data as specified by their frequency (F) and wavenumber (K) (Hatton et al. 1986). To achieve this a shot section is transformed from the time-space domain where it is recorded to frequency-wavenumber domain by a two dimensional fourier transform. The reason for this approach is that events in the shot section with different velocities will appear in different places in the FK-domain. The surface wave will in the FK-domain occur on a line

$$V_{\text{surf}} = F/K.$$

A reflection will have a high apparent velocity, and will therefore appear at low wavenumbers. Fig. 9 (a,b) shows a synthetic shot section in both time-space domain and FK-domain.

The procedure in FK-filtering is

- preprocess the shot section
- transform it into the FK-domain
- cut out the areas in the FK-domain that contains the unwanted data
- transform back to the time-space domain
- continue with processing e.g. CDP-stacking

Fig. 9 (c) shows a synthetic example of a FK-filtered shot section.

To choose the best preprocessing and the parameters for the FK-filter, a number of test were carried out, both on synthetic data to test the method, and on real data. The preprocessing consists of:

The shot sections are band-pass filtered to avoid spatial aliasing. The distance between the recording geophones is 10 m, and to get a sufficient sampling in the spatial direction the apparent wavelength of any signal must be larger than 20 m. The ground coupled airblast has velocity 340 m/s, and will be spatially aliased at frequencies above 17 Hz. This event is therefore muted out. The 'slowest' arrival left in the data is the surface wave, with velocity ~2.0 km/s, which means that it will be spatially aliased at frequencies above 100 Hz. The bandpass filter used is 20 - 100 Hz

The fourier transform in the space direction is done on 60 samples recorded on 60 different geophones at the same time. The response of the geophone is dependent on the site, and the sampling of the originally continuous signal in space is not continuous. The traces recorded on each geophone are equalized so that the mean amplitude is the same for all sites.

The fourier transform is carried out by a FFT routine (Fast Fourier Transform) which requires input arrays of the power of 2. For the time direction 1024 samples were used, but in the space direction only 60 samples were available. These were therefore tapered down to zero at the smallest and largest offsets, and extended with zeroes to an array of 128 samples. This process degrades the shot section, as it is necessary to involve 60 % of the data. This means loss of information. The only way to avoid this is to record on more than 60 channels. A taper is also applied in the time direction, but is much less significant here, due to the larger number of samples. The taper must be applied to obtain continuity in the arrays.

The recorded shot section contains - of course- noise as well as signal. The noise is also filtered, meaning dips let through the FK-filter-sub horizontal- are enhanced. This can give the FK-filtered shot section a 'stripy' look. Therefore only the part of the FK-spectrum with negative wavenumbers is filtered, as the geometry used only gives rise to surface- and S-waves with negative wavenumbers (fig. 9 b).

Fig. 9 (d,e) shows an example of a real shot section before and after FK-filtering. If compared with the synthetic example in fig. 9 a&c it is clear that there must be a component in the data that was not modelled by the synthetic shot section. There seems to be a residue of the surface- and S-wave consisting of near horizontal, rather high amplitude short stripes. A number of tests with synthetic data revealed that static time shifts (static corrections) on the traces can model the residual left in the real data (fig. 9 f&g). To find these corrections a search procedure was carried out to find the optimum set of correction , assigning one correction to each geophone site and shot. This search required the data to be timeshifted - reduced time- so the surface wave (or the S- or direct-wave) apart from the correction is horizontal. The known time shift applied before the search is

$$t_{\text{red}} = t - \frac{\text{offset}}{\text{vel}}$$

In order for the search to find the corrections, the velocity used must be correct over the whole profile. Variations in this velocity along the profile ought to be taken into account, and this might be a reason why we did not succeed in finding a set of corrections that eliminates the residual left after FK-filtering. A section stacked from the FK-filtered shot section turns out to be dominated by these residuals, therefore we do not present any FK-filtered stack.

12. Deep stack

To see if we could detect any reflectors beneath 400 ms a stacked section was produced (fig. 10) which extends to 1.5 s TWT. For comparison, a stacked section from the parameter test profile is shown in fig. 11. This profile strikes the main profile approximately at right angle (fig. 1). The processing steps for the two stacks were the same, namely:

- demultiplexing and gain recovering
- CDP-sorting
- muting of ground-coupled air-blast
and of surface- and direct wave (test profile)
- band-pass filtering 40-250 Hz
- equalizing the power of the traces
- NMO-correcting with a reasonable velocity function
(5.2 km/s at the surface, increasing to 6.0 km/s at depth)
- displaying with AGC (Automatic Gain Control)

Due to the mute cutting of the surface wave and above events, the test stack does not give a meaningful picture above 300 ms TWT. The main stack has been muted in another way, but the resolution of shallow events is still poor.

A reflecting band can be seen on both stacks, beginning at 0.5 s TWT (approximately corresponding to 1.5 km), extending to 1.0 s TWT. This feature indicates not a single, well-defined reflector, but a complex reflecting zone.

13 Summary and conclusions

One of our main efforts has been to produce a stack where zone 2 can be followed along the profile. This has not been successful, in spite of a variety of different approaches (careful muting, FK-filtering, semblance, stacking etc.). These procedures have been necessary because of low amplitude reflection and high amplitude surface- and S-waves. If these high amplitude events are not removed from the data before stacking, they will degrade it to an extent that makes it impossible to see anything else.

The zone is also difficult to see on the shot sections. It cannot be a strongly reflecting zone. The reflectivity of a fracture zone depends on the velocities and densities of the zone and the rock surrounding it. Unfortunately we have no information of the elastic properties of zone 2, and cannot judge the reflection coefficient. The fact that we do not see zone 2 and know that it is there all the same is a reminder that we may see a fracture zone, but we do not necessarily see it.

The steeply dipping Brändan zone is crossed by the profile, and is seen on a number of shot sections (fig. 3 (g)). It appears to be more reflective than zone 2.

An attempt to enhance reflections by calculating semblance along hyperbolas did not improve on the appearance of zone 2, but showed a feature that can be interpreted as a reflection. There are no boreholes where we would expect to see it, and without further information, we cannot determine its nature.

On fig. 10 reflections from depths below 400 ms are seen, but as a broad band of coherent energy in the time window 0.5-1.0 sec, corresponding to approximately 1500-3000 m depth.

References

- Ahlbom,K., Andersson,P., Ekman,L., Gustafsson,E., Smellie,J. and Tullborg,E-L. 1986 : Preliminary investegations of fracture zones in Brändan area, Finnsjön study site. SKB Technical Report 86-05
- Dahl-Jensen,T. and Palm,H. 1987 : Reflection seismic parameter test at Finnsjön may 87. SKB AR 87-19
- Ekman,L and Jacobsson,J-Å 1987 : Reflexionseismisk profil i Brändan området, Finnsjön. Dokumentation av sprängborrhål. SKB AR 87-15
- Hatton,L., Worthington,M.H. and Makin,J. 1986 : Seismic Data Processing. Blackwell Scientific Publications
- Hubral,P. and Krey,T. 1980 : Interval Velocities from Seismic Reflection Time Measurement. SEG Publications, Oklaholma
- Knapp,R.W. and Steeples,D.W. 1986 : High resolution common-depth-point relection profiling: Field acquisition parameter design. Geophysics, vol 51 no. 2 p. 283-294
- Kearey,P. and Brooks,M. 1984 : An Introduction to Geophysical Exploration. Blackwell Scientific Publications

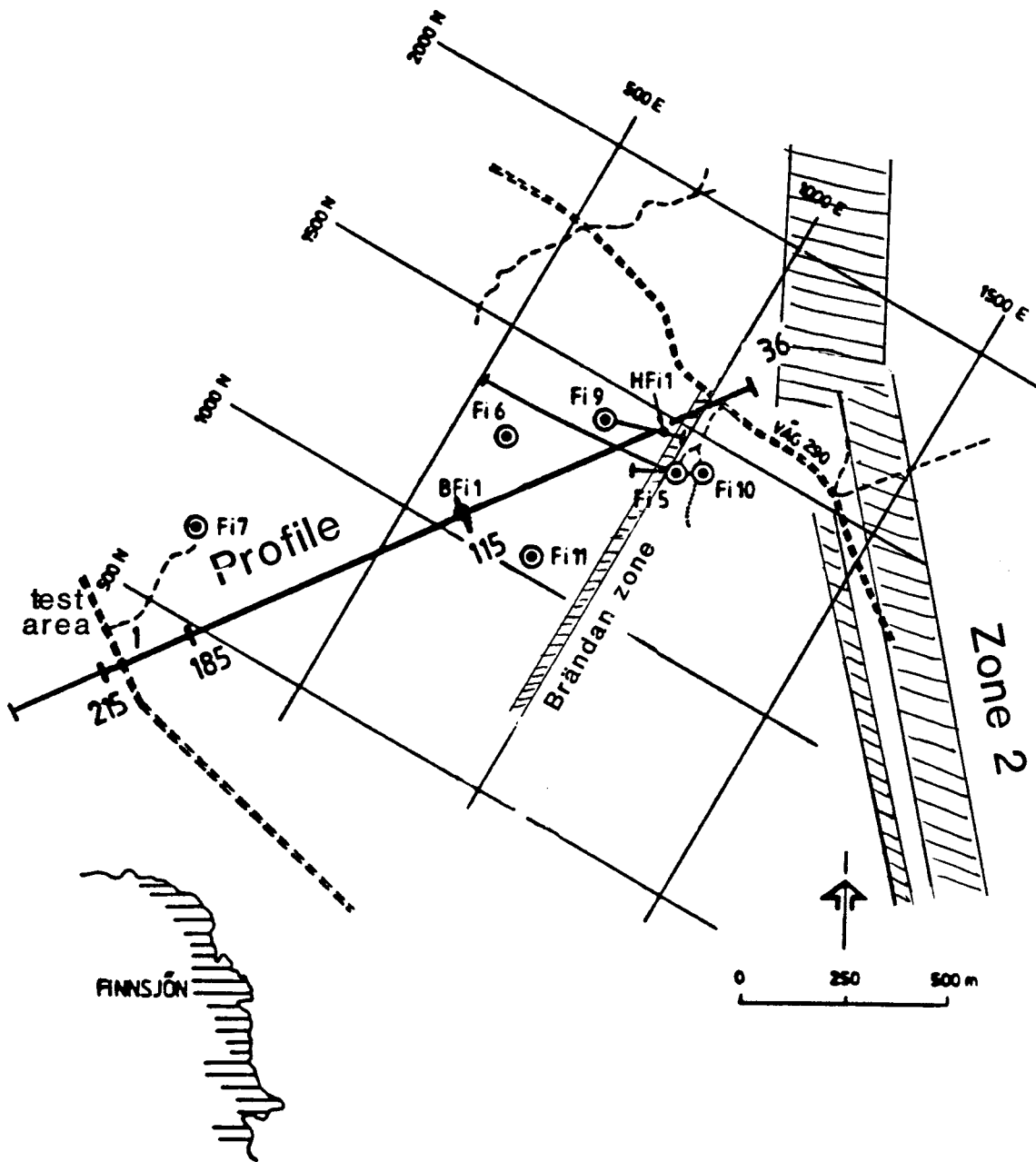
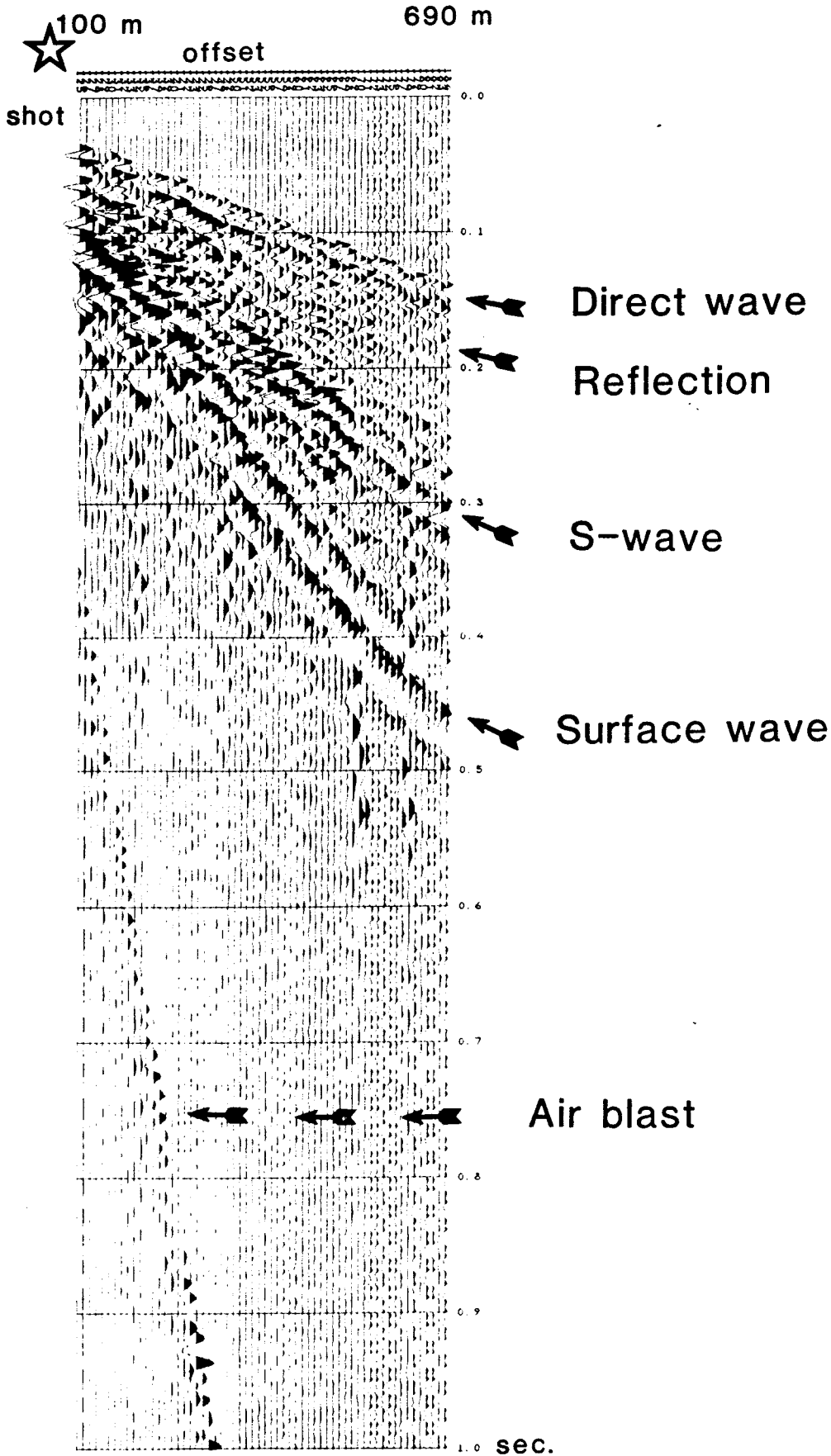


Fig. 1 Map showing the reflection seismic profile, the bore holes in the area, zone 2 and the Brändan zone, and the test area.

FINN-1-11401

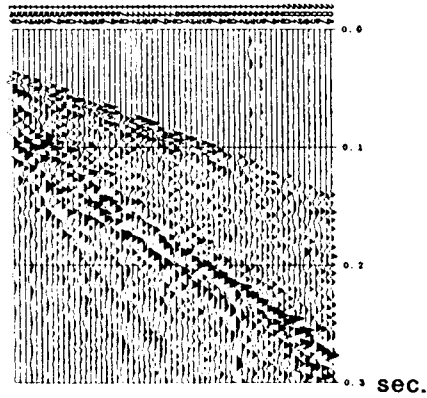
BANDPASS 20-220 HZ
SCALING BY MEAN AMPLITUDE

Fig. 2 To illustrate the various events on a typical shotsection from the profile, shot 11401 showing the arrivals.



FINN-1-13800

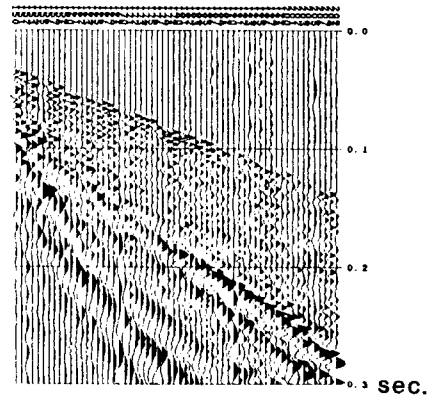
BANDPASS 20-220 HZ
SCALING BY MEAN AMPLITUDE



a

FINN-1-13900

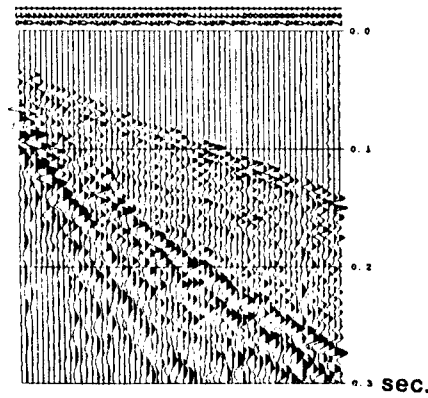
BANDPASS 20-220 HZ
SCALING BY MEAN AMPLITUDE



b

FINN-1-12700

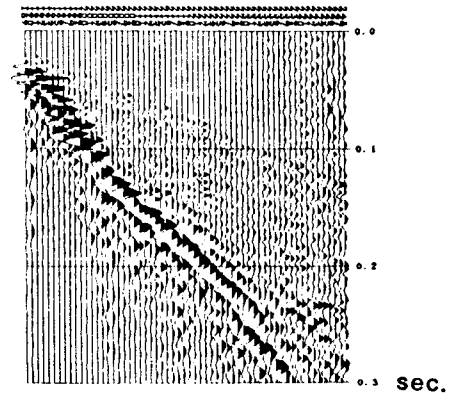
BANDPASS 20-220 HZ
SCALING BY MEAN AMPLITUDE



e

FINN-1-18500

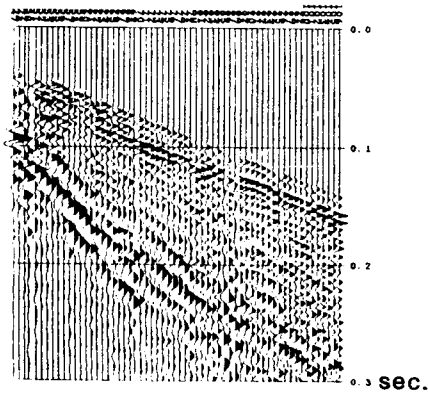
BANDPASS 20-220 HZ
SCALING BY MEAN AMPLITUDE



f

FINN-1-3600

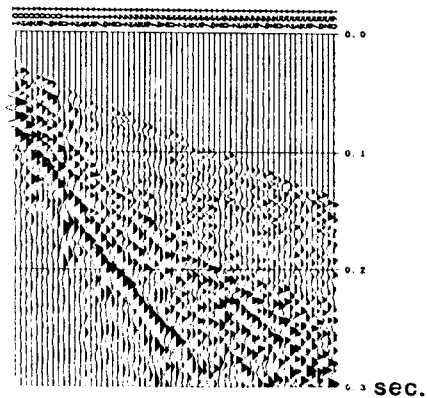
BANDPASS 20-220 HZ
SCALING BY MEAN AMPLITUDE



c

FINN-1-9000

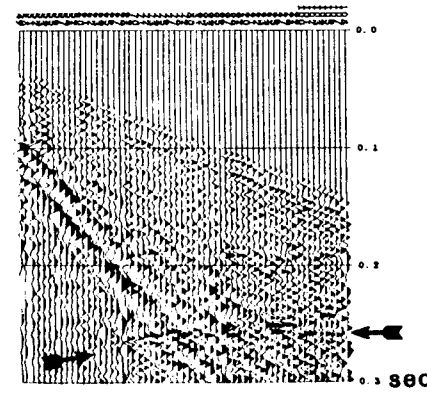
BANDPASS 20-220 HZ
SCALING BY MEAN AMPLITUDE



d

FINN-1-4001

BANDPASS 20-220 HZ
SCALING BY MEAN AMPLITUDE



g

Fig. 3 Shot sections.
a: Shot section from a shot fired 1.20 m into bedrock covered by 0.80 m soil.
b: Shot section from a shot fired 0.20 m into bedrock covered by 2.60 m soil.
c: Shot section from the beginning of the profile. Zone 2 is here close to the surface.
d, e: Shot sections from the central part of the profile.
f: Shot section from the end of the profile.
g: Shot section where zone 1, the Brandon Fracture Zone, appears as a marked event.

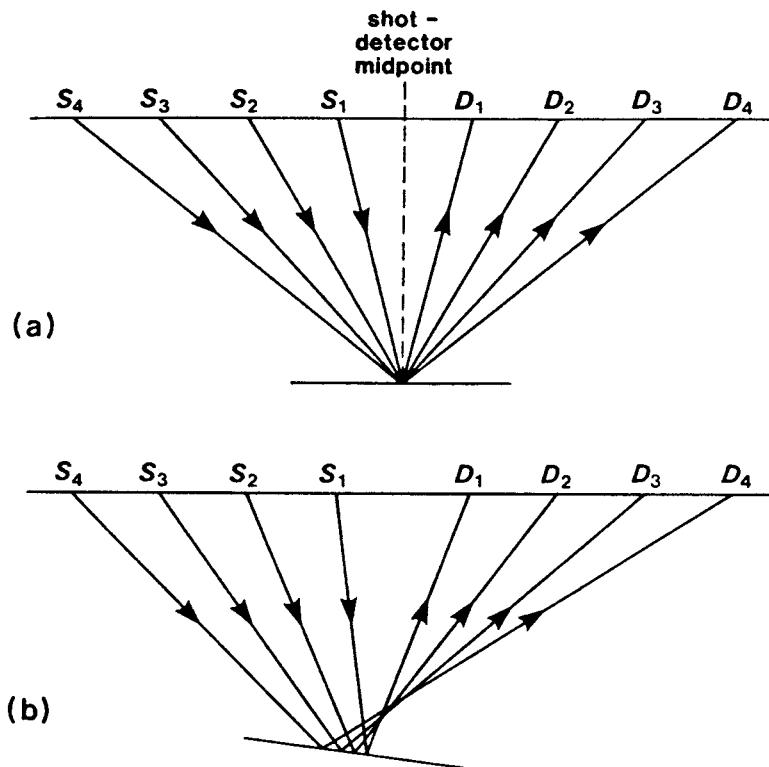


Fig. 4 CDP-profiling involves the addition of a number of traces, after a correction for varying offset (NMO-correction). The figure shows the ray paths of a collection of traces belonging to the same CDP-gather. (a) is a horizontal reflector, (b) is the case of a dipping reflector. Along the profile in the Finnsjö area, the CDP-gathers normally contain 25-30 traces. From Krearey and Brooks 1984

FINN-1 CDP NO = 150

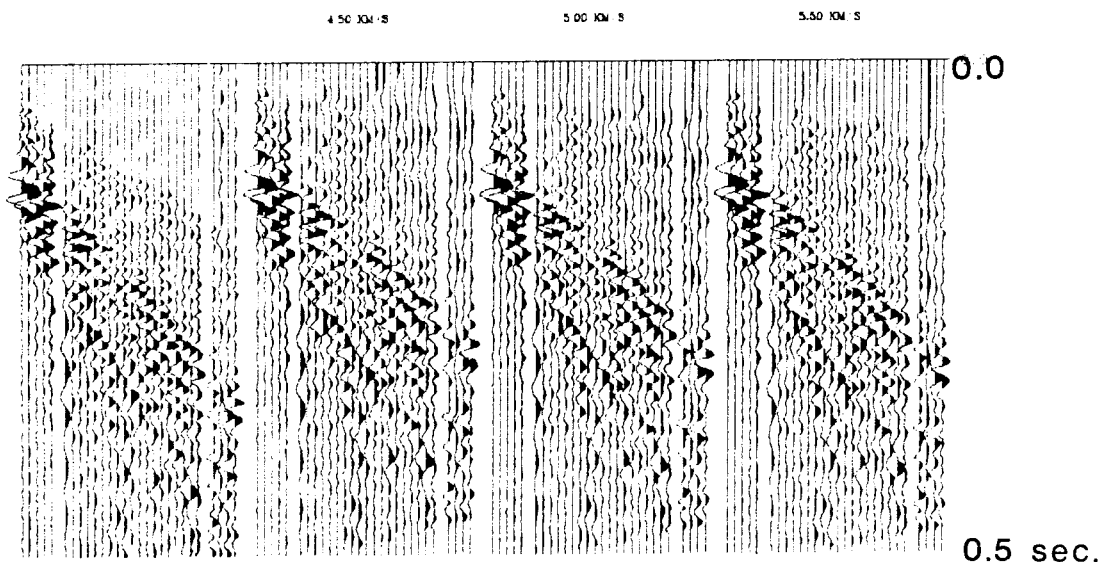


Fig. 5 CDP-gather 150 is shown first with no NMO-correction, then with 3 different velocities (4.4 5.0 5.5 km/s) The traces at largest offset have a lower frequency content after NMO-correction, specially at early times.

FINN-1 SHOTNO 13500

CHANNELS 24 TO 34, 0 MSEC TO 4096 MSEC

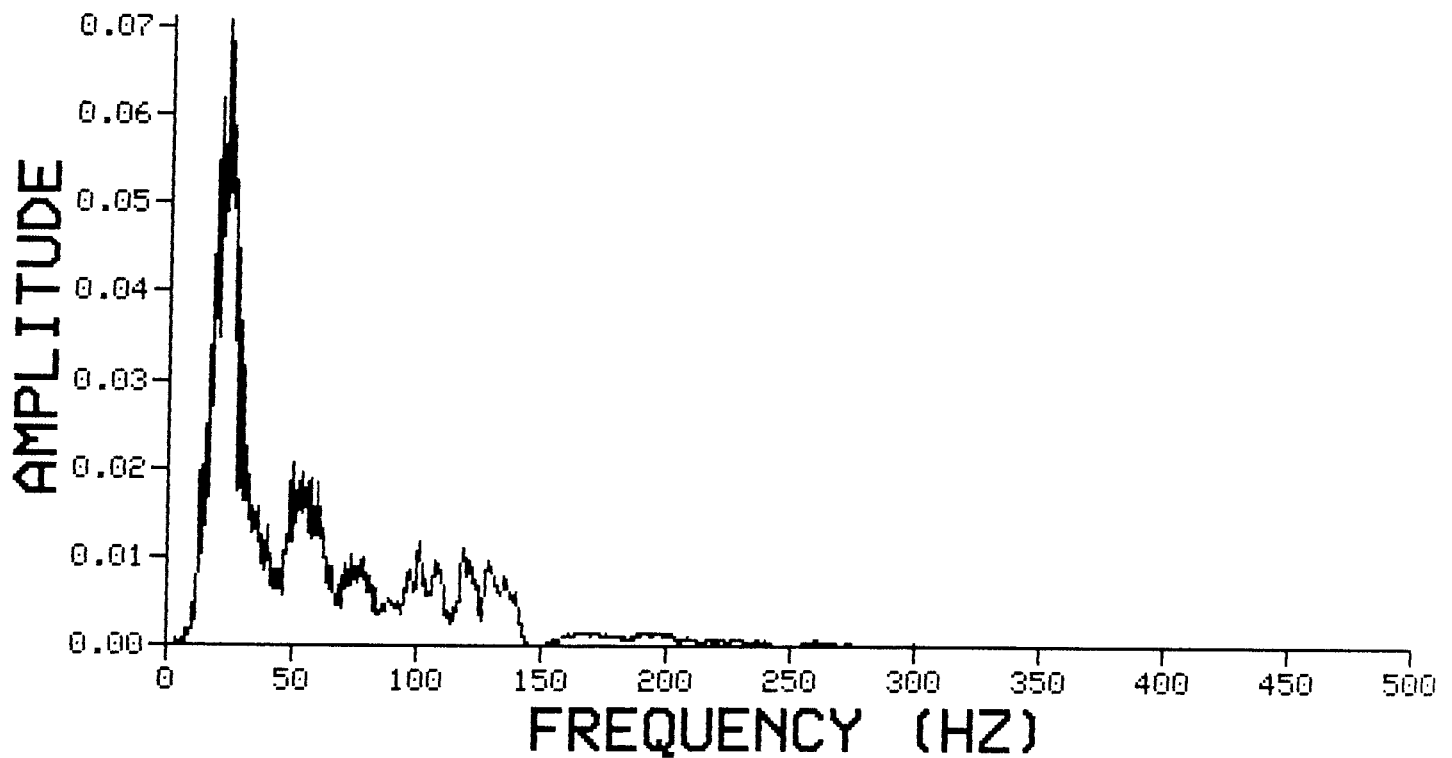
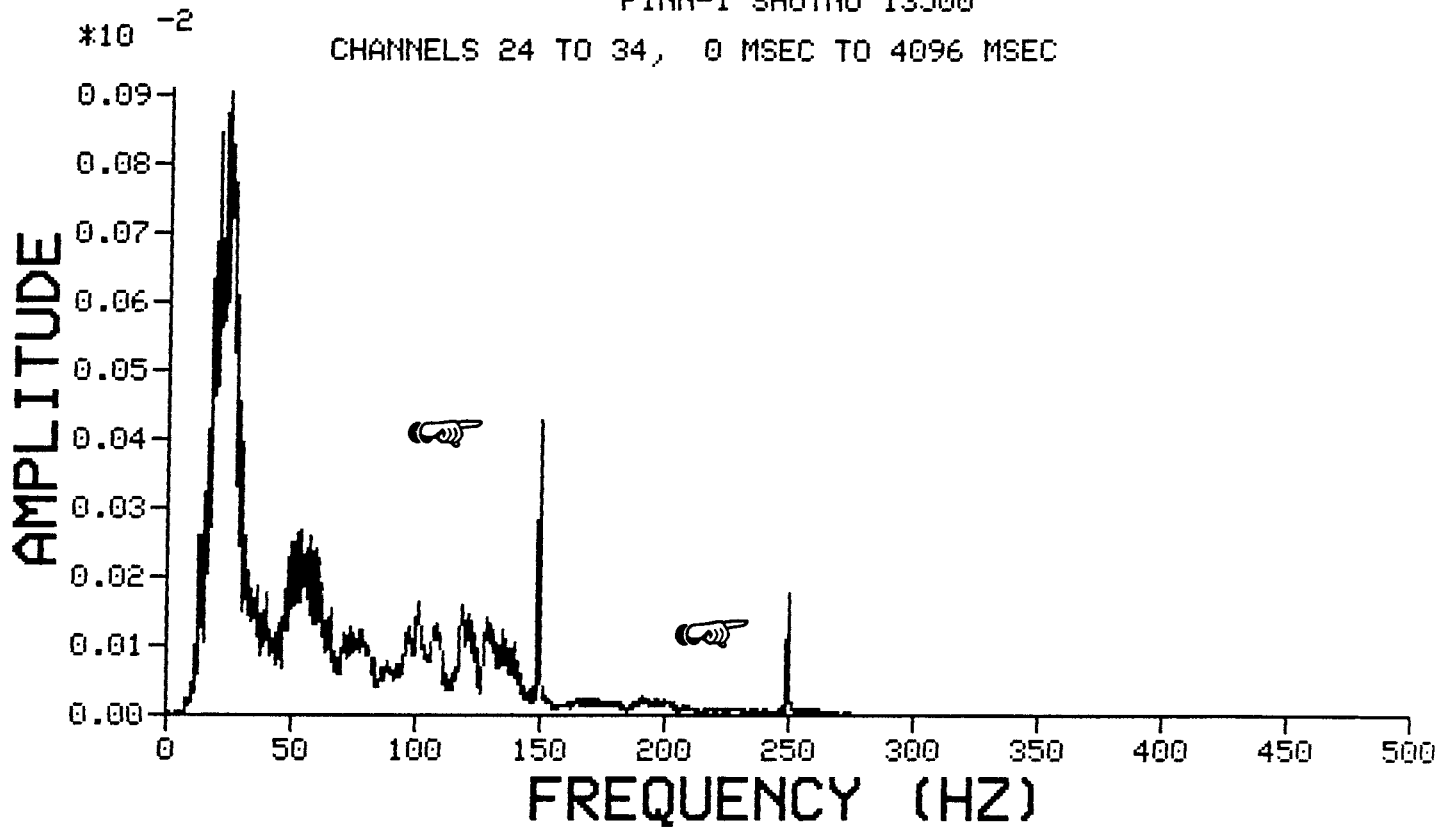
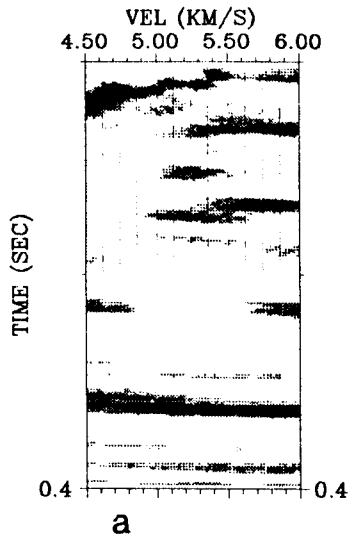
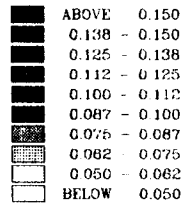


Fig. 6 Several geophone sites were problematic because of 50 Hz noise and over tones (150 and 250 Hz). The figure shows the frequency content of a shotsection before and after notchfiltering.

13:15 26/06 87

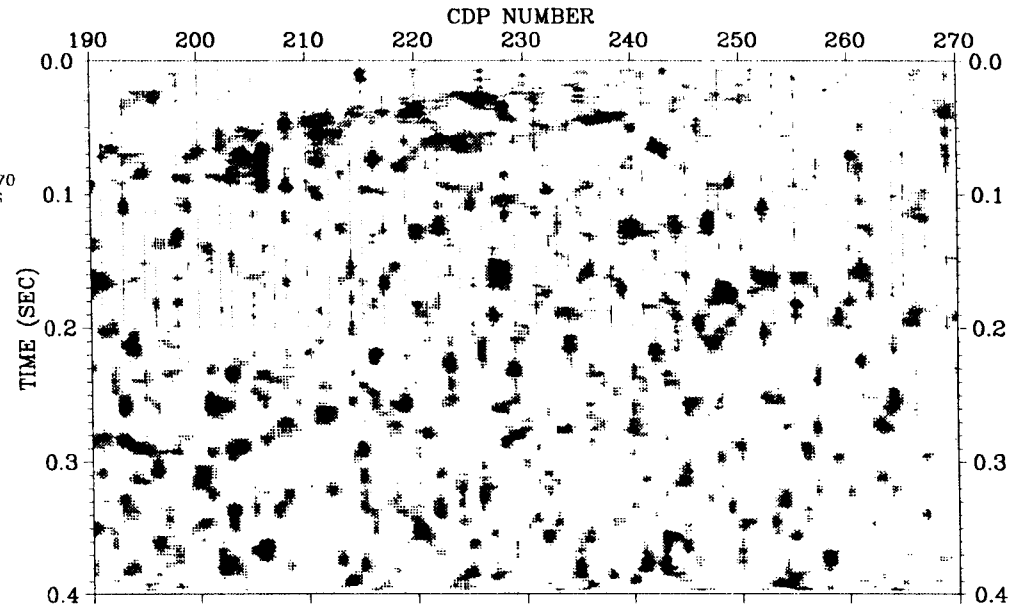
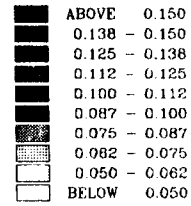
FINN-1
CDP NUMBER 200
FOLD = 26
OFFSET RANGE
109 - 661 M
TIME GATE = 10 MS



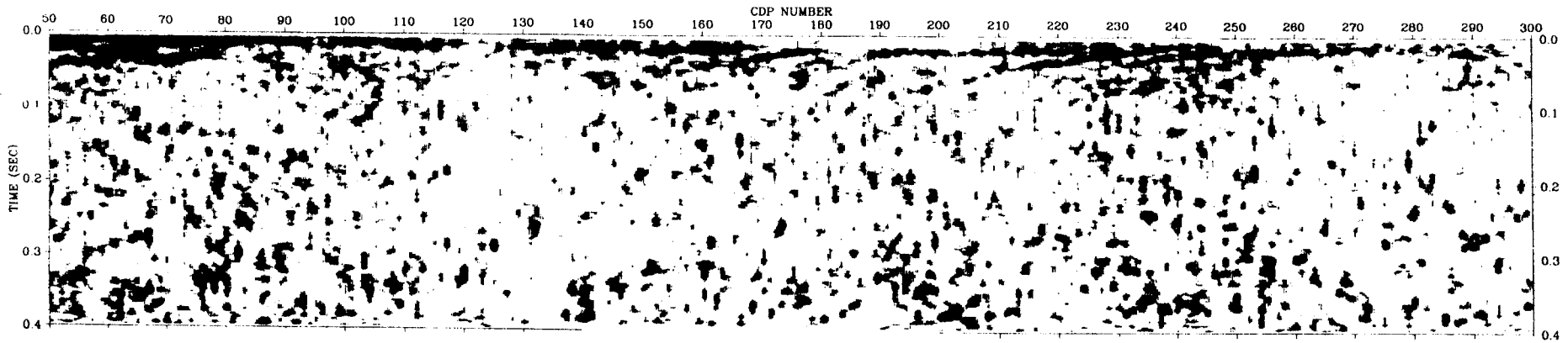
a

09:34 26/06-87

CDP NUMBER 190 - 270
VELOCITY = 5.75 KM/S
TIME GATE = 10 MS



c



b

Fig. 7 Semblance analysis.

a: Velocity analysis of a CDP-gather.

b: Semblance stack with stacking velocity 5.25 km / s.

c: Part of semblance stack, stacking velocity 5.75 km / s.

FINN-1-13900

BANDPASS 20-220 HZ

MUTE 1.80 - 2.80 KM/S 110 RESP 30 SAMPLES DELAY

SCALING BY MEAN AMPLITUDE

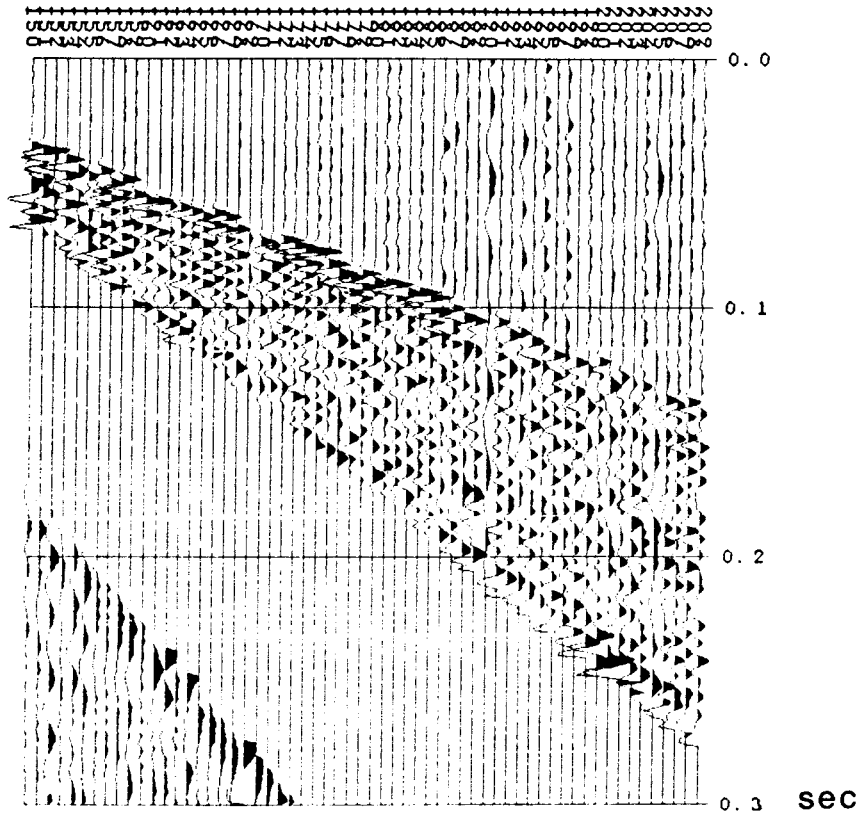


Fig. 8 Shot section 13900 with a mute applied. All data values between velocities 1.8 - 2.8 km/s were set to zero to remove the S- and surface wave.

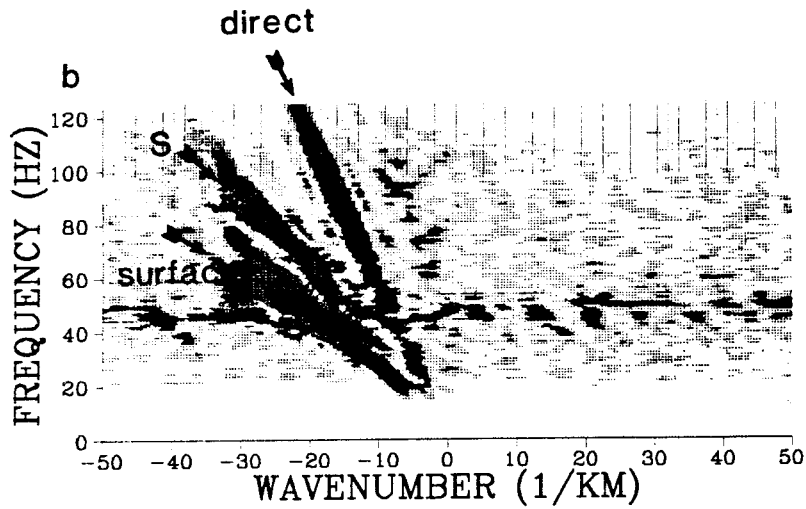
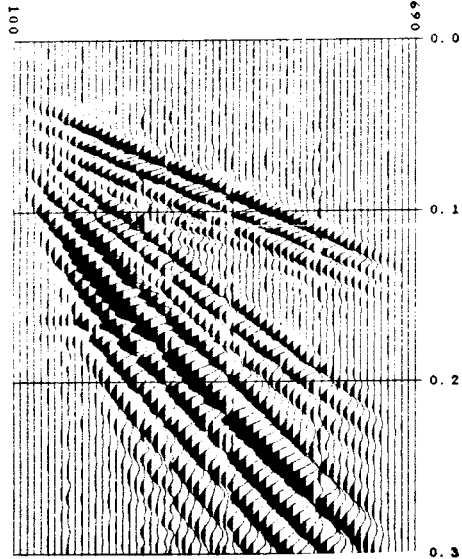
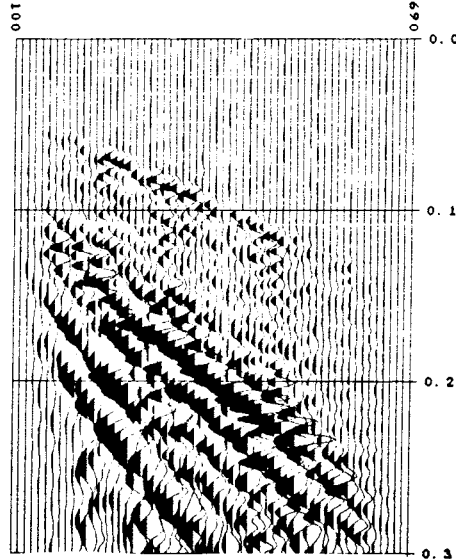


Fig. 9 FK-filtering. (a) is a synthetic shot section containing direct wave, S-wave, surface wave and two reflections. Noise is added to each trace, with varying strength. The geometry is the same as for the real shots. (b) is a FK-spectrum of (a), (c) is FK-filtered to remove the S-wave and surface wave. (d) is shot section 14701, (e) is FK-filtered. (f) is the same synthetic shot section as (a), but with static correction ranging between 0-5 ms. (g) shows (f) with FK-filter applied, and demonstrates the residue left, as it is on the real shot sections.

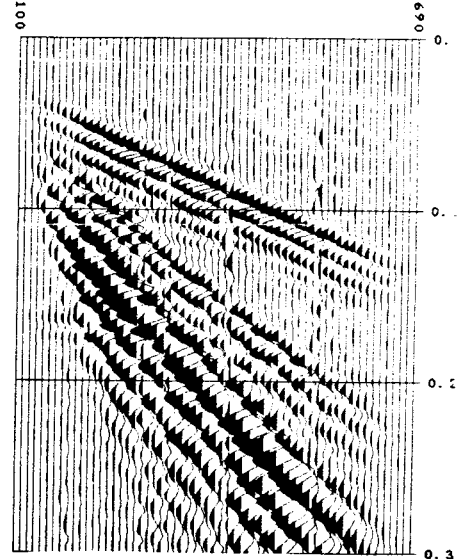
a SYNTHETIC DATA
BANDPAS 20-100 HZ
MUTE 0.00-0.40 KM/S
NO SCALING



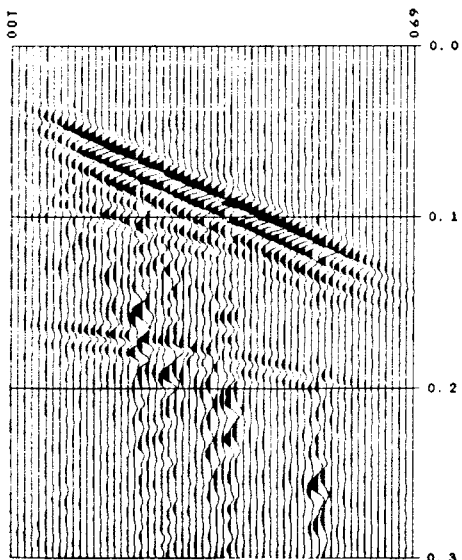
d SHOTNUMBER 14701
BANDPAS 20-100 HZ
MUTE 0.00-0.40 KM/S
NO SCALING



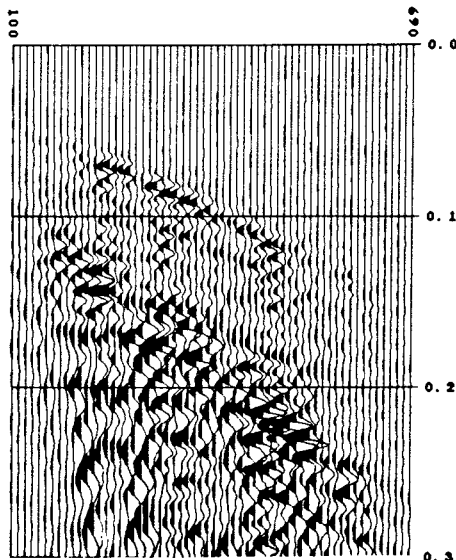
f SYNTHETIC DATA
BANDPAS 20-100 HZ
MUTE 0.00-0.40 KM/S
NO SCALING



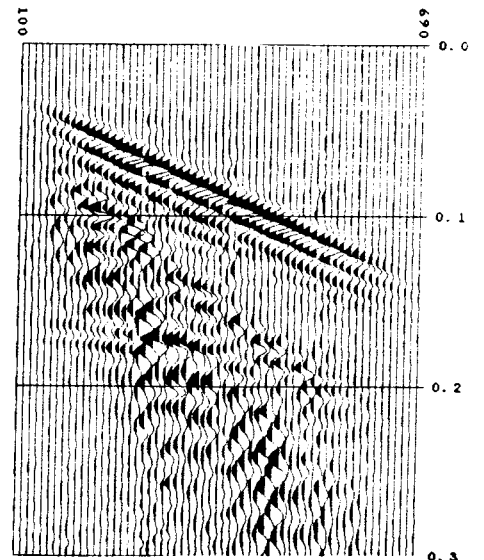
c SYNTHETIC DATA
BANDPAS 20-100 HZ
MUTE 0.00-0.40 KM/S
FK-FILTER 1.50-4.20 KM/S
NO SCALING



e SHOTNUMBER 14701
BANDPAS 20-100 HZ
MUTE 0.00-0.40 KM/S
FK-FILTER 1.50-4.20 KM/S
NO SCALING



g SYNTHETIC DATA
BANDPAS 20-100 HZ
MUTE 0.00-0.40 KM/S
FK-FILTER 1.50-4.20 KM/S
NO SCALING



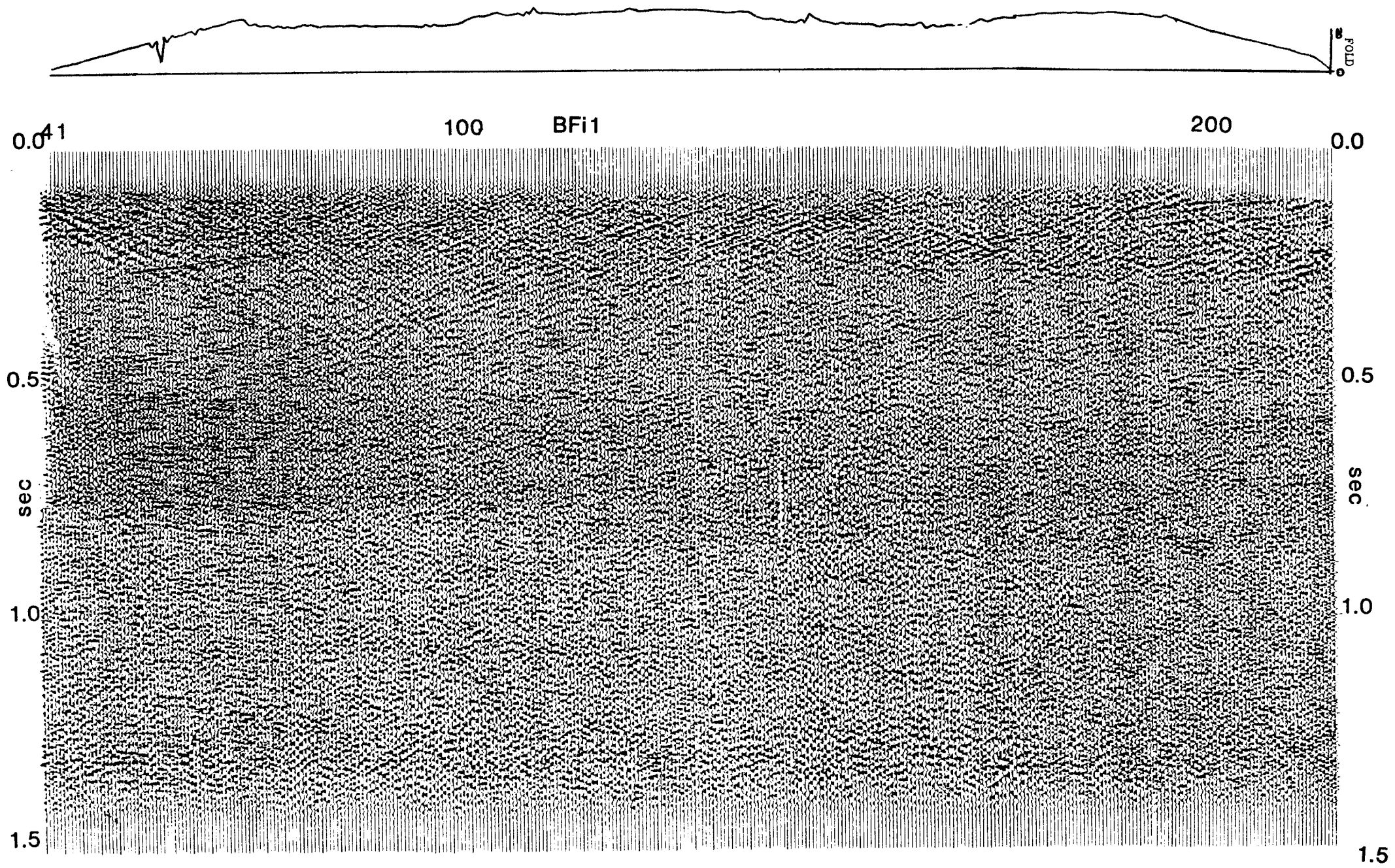


Fig. 10 A stacked section concentrating on TWT below 400 ms. The numbers at the top refer to geophone station numbers (see fig 1). The curve at the top shows the number of traces in the CDP-gathers. The event seen at app. 0.3 sec in the beginning of the profile is a processing artifact, and no reflector.

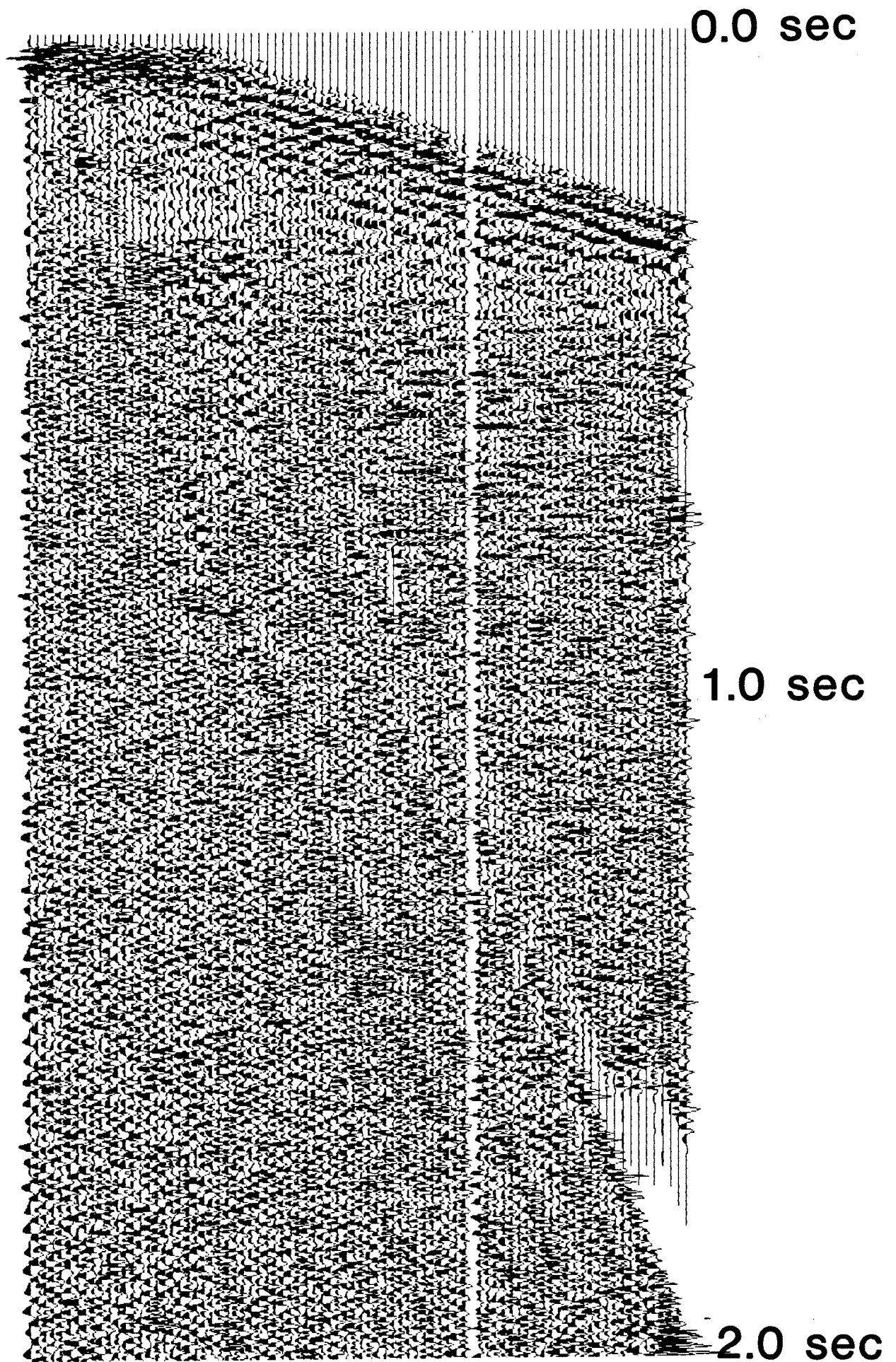


Fig. 11 Stacked section from the short profile shot during the parameter test. The seismic charge was here 100g, the rest of the parameters were identical to profile 1. The processing parameters are set to enhance the section below 3-400 ms depth.

List of SKB reports

Annual Reports

1977-78

TR 121

KBS Technical Reports 1 – 120.

Summaries. Stockholm, May 1979.

1979

TR 79-28

The KBS Annual Report 1979.

KBS Technical Reports 79-01 – 79-27.

Summaries. Stockholm, March 1980.

1980

TR 80-26

The KBS Annual Report 1980.

KBS Technical Reports 80-01 – 80-25.

Summaries. Stockholm, March 1981.

1981

TR 81-17

The KBS Annual Report 1981.

KBS Technical Reports 81-01 – 81-16.

Summaries. Stockholm, April 1982.

1982

TR 82-28

The KBS Annual Report 1982.

KBS Technical Reports 82-01 – 82-27.

Summaries. Stockholm, July 1983.

1983

TR 83-77

The KBS Annual Report 1983.

KBS Technical Reports 83-01 – 83-76

Summaries. Stockholm, June 1984.

1984

TR 85-01

Annual Research and Development Report 1984

Including Summaries of Technical Reports Issued during 1984. (Technical Reports 84-01 – 84-19)
Stockholm June 1985.

1985

TR 85-20

Annual Research and Development Report 1985

Including Summaries of Technical Reports Issued during 1985. (Technical Reports 85-01-85-19)
Stockholm May 1986.

1986

TR86-31

SKB Annual Report 1986

Including Summaries of Technical Reports Issued during 1986
Stockholm, May 1987

Technical Reports

1987

TR 87-01

Radar measurements performed at the Klipperås study site

Seje Carlsten, Olle Olsson, Stefan Sehlstedt,
Leif Stenberg
Swedish Geological Co, Uppsala/Luleå
February 1987

TR 87-02

Fuel rod D07/B15 from Ringhals 2 PWR: Source material for corrosion/leach tests in groundwater

Fuel rod/pellet characterization program part one

Roy Forsyth, Editor
Studsvik Energiteknik AB, Nyköping
March 1987

TR 87-03

Calculations on HYDROCOIN level 1 using the GWHRT flow model

Case 1 Transient flow of water from a borehole penetrating a confined aquifer

Case 3 Saturated-unsaturated flow through a layered sequence of sedimentary rocks

Case 4 Transient thermal convection in a saturated medium

Roger Thunvik, Royal Institute of Technology,
Stockholm
March 1987

TR 87-04

Calculations on HYDROCOIN level 2, case 1 using the GWHRT flow model

Thermal convection and conduction around a field heat transfer experiment

Roger Thunvik
Royal Institute of Technology, Stockholm
March 1987

TR 87-05

Applications of stochastic models to solute transport in fractured rocks

Lynn W Gelhar
Massachusetts Institute of Technology
January 1987

TR 87-06

Some properties of a channeling model of fracture flow

Y W Tsang, C F Tsang, I Neretnieks
Royal Institute of Technology, Stockholm
December 1986

TR 87-07

Deep groundwater chemistry

Peter Wikberg, Karin Axelsen, Folke Fredlund
Royal Institute of Technology, Stockholm
June 1987

TR 87-08

An approach for evaluating the general and localized corrosion of carbon steel containers for nuclear waste disposal

GP March, KJ Taylor, SM Sharland, PW Tasker
Harwell Laboratory, Oxfordshire
June 1987

TR 87-09

Piping and erosion phenomena in soft clay gels

Roland Pusch, Mikael Erlström,
Lennart Börgesson
Swedish Geological Co, Lund
May 1987

TR 87-10

Outline of models of water and gas flow through smectite clay buffers

Roland Pusch, Harald Hökmark,
Lennart Börgesson
Swedish Geological Co, Lund
June 1987

TR 87-11

Modelling of crustal rock mechanics for radioactive waste storage in Fennoscandia—Problem definition

Ove Stephansson
University of Luleå
May 1987

TR 87-12

Study of groundwater colloids and their ability to transport radionuclides

Kåre Tjus* and Peter Wikberg**
*Institute for Surface Chemistry, Stockholm
**Royal Institute of Technology, Inorganic
Chemistry Stockholm
March 1987